

---

---

## PICTORIAL ESSAY

---

---

# Multimodality Imaging Spectrum of Extranodal Lymphoma: A Pictorial Review

JAWK Tang, BST Leung, DTF Lee, HT Sung, CS Cheng

*Department of Radiology, Pamela Youde Nethersole Eastern Hospital, Chai Wan, Hong Kong*

### ABSTRACT

*Extranodal lymphoma is relatively uncommon and has a wide radiological spectrum in various organs. In this pictorial review, the radiological features across various imaging modalities and the differential diagnoses of extranodal lymphomatous involvement of different organs are described.*

*Key Words: Lymphoma, extranodal NK-T-cell; Lymphoma, large B-cell, diffuse; Lymphoma, non-Hodgkin*

## 中文摘要

### 淋巴結外淋巴瘤的多模態成像表現：圖像綜述

鄧永健、梁肇庭、李騰飛、宋咸東、鄭志成

淋巴結外淋巴瘤不常見，並且在不同器官中具有不同的放射學表現。此圖像綜述描述淋巴結外淋巴瘤在各種成像方式中的放射學特徵以及它在不同器官的鑑別診斷。

### INTRODUCTION

Lymphoma is a form of lymphoproliferative disorder with various subtypes which are broadly classified into non-Hodgkin lymphoma and Hodgkin lymphoma. Extranodal lymphoma is uncommon, but various organs can be affected. Some typical radiological findings are well described in the radiology literature, whereas others are non-specific. In this article, the imaging spectrum of extranodal lymphoma is described.

### DEFINITION

Non-Hodgkin and Hodgkin lymphoma can both involve extranodal organs with the former histological group being more common. Extranodal disease is commonly encountered as secondary lymphomatous involvement, and outnumbers primary extranodal lymphoma by one or two orders of magnitude.<sup>1</sup> Primary extranodal lymphoma should be confined to a single extranodal organ and lymph nodes in the close proximity. The

---

*Correspondence: Dr JAWK Tang, Department of Radiology, Pamela Youde Nethersole Eastern Hospital, Chai Wan, Hong Kong.  
Email: tangwingkin2000@gmail.com*

Submitted: 30 Jul 2017; Accepted: 12 Oct 2017.

Disclosure of Conflicts of Interest: All authors have disclosed no conflicts of interest.

Funding/Support: This research received no specific grant from any funding agency in the public, commercial, or not-for-profit sectors.

Ethics Approval: This study was conducted in accordance with the Declaration of Helsinki and the guidelines of the local ethics committee. All patients provided consent.

presence of additional primary nodal sites or extranodal organ involvement elsewhere would define the condition as secondary extranodal lymphoma.<sup>1</sup> The main focus in this article is extranodal involvement in non-Hodgkin lymphoma.

## NERVOUS SYSTEM

### Central Nervous System

Secondary lymphomatous involvement in the central nervous system (CNS) is relatively common, accounting for 10% to 15% of cases. In contrary, primary CNS lymphoma is rare and accounts for only 1% of all non-Hodgkin lymphoma.<sup>2,3</sup> Typical sites of involvement in the brain are corpus callosum, deep grey matter, and periventricular and subependymal regions. The radiological patterns of CNS lymphoma vary between immunocompetent and immunocompromised patients; the latter shows predilection to ring-like enhancement resulting from central necrosis of the lesion, whereas such a finding is uncommon in immunocompetent patients.<sup>4</sup> In immunocompromised patients, ring-like enhancement should raise suspicion for other differentials, including toxoplasmosis, fungal abscess, tuberculoma, and rarely as a manifestation of cerebral cytomegalovirus infection.<sup>5</sup> Furthermore, bulky tumour involvement at the corpus callosum without evidence of tumour necrosis is also characteristic of CNS lymphoma. Other differentials, such as gliomas, seldom present without necrotic change when the tumour size becomes

substantial.<sup>6</sup> Other general imaging features reflect its hypercellularity and low water content; therefore, lesions appear hyperdense on non-enhanced computed tomography (CT) and T2 iso- to hypo-intense with restricted diffusion on magnetic resonance imaging (MRI) [Figure 1].<sup>2</sup> MR spectroscopy can demonstrate evidence of increased cell turnover and decreased neuronal activity, ie, high choline peak, reversed choline / creatine ratio, and markedly low N-acetylaspartate.<sup>2</sup> These MR spectroscopy features are not pathognomonic for lymphoma; other pathologies such as glioma and cerebral metastasis can also demonstrate similar findings. Newer MRI techniques with perfusion-weighted imaging have been suggested to provide additional features to distinguish between lymphoma and other brain tumours. Lymphoma shows lower relative cerebral blood volume ratio than other brain tumours. This is particularly helpful in differentiating lymphoma from high-grade glioma, because the latter tends to demonstrate high relative cerebral blood volume ratio.<sup>7</sup>

### Peripheral Nervous System

Neurolymphomatosis represents intraneural lymphomatous infiltration of peripheral nerves. Although it usually occurs in the context of systemic lymphoma, only 20% of neurolymphomatosis has an established history of systemic lymphoma at the time of the diagnosis of peripheral nerve involvement.<sup>8</sup> Diffuse large B-cell lymphoma constitutes majority of the

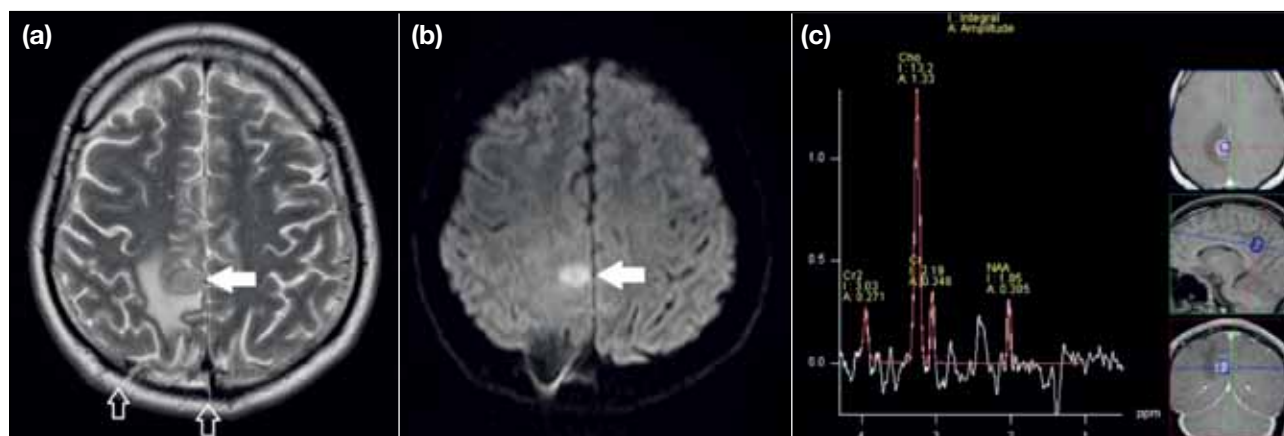


**Figure 1.** Primary central nervous system lymphoma. (a) Axial T2-weighted magnetic resonance image shows a focal mass at right paramedian parietal lobe with T2 signal isointense to the adjacent grey matter (white arrow) and perifocal T2 hyperintense signal due to oedema. Recent right parietal craniotomy for biopsy of this lesion is evident (empty white arrows). (b) Diffusion-weighted image at b1000 shows high signal intensity of the lesion (white arrow), together with low signal in apparent diffusion coefficient mapping (not shown), this compatible with restricted diffusion related to high cellularity. (c) Magnetic resonance spectroscopy of this lesion shows high choline peak, reversed choline / creatine ratio and low N-acetylaspartate, suggestive of increased cell turnover and decreased neuronal activity.

histological subtypes in neurolymphomatosis, although both T-cell and B-cell lymphomas can be encountered in neurolymphomatosis.<sup>9</sup> Patients usually present with pain and sensorimotor deficit of the involved nerve. On MRI, nodular or fusiform enlargement of the nerve and mild to moderate contrast enhancement would be present (Figure 2).<sup>10</sup> Other differentials to consider in the context of known history of lymphoma include infection (eg, herpes zoster), neuropathy of various aetiologies (eg, vinca alkaloids chemotherapy-related, radiation-induced and nerve root compression, Guillain-Barre syndrome, or chronic idiopathic demyelinating polyradiculoneuropathy), and lymphoma-associated vasculitis and amyloidosis.<sup>9</sup>

## HEAD AND NECK

### Orbit

Primary orbital tumours are predominantly lymphoproliferative lesions occurring in adults aged  $\geq 60$  years; majority of primary orbital tumours are lymphoma.<sup>11</sup>

The lacrimal gland is the most common site of lymphomatous involvement in the orbit. The most common histological subtype of primary orbital lymphoma is mucosa-associated lymphoid tissue lymphoma (Figure 3).<sup>2</sup> Patient with orbital lymphoma may present with proptosis due to mass effects of the lesion. Radiological appearance of orbital lymphoma

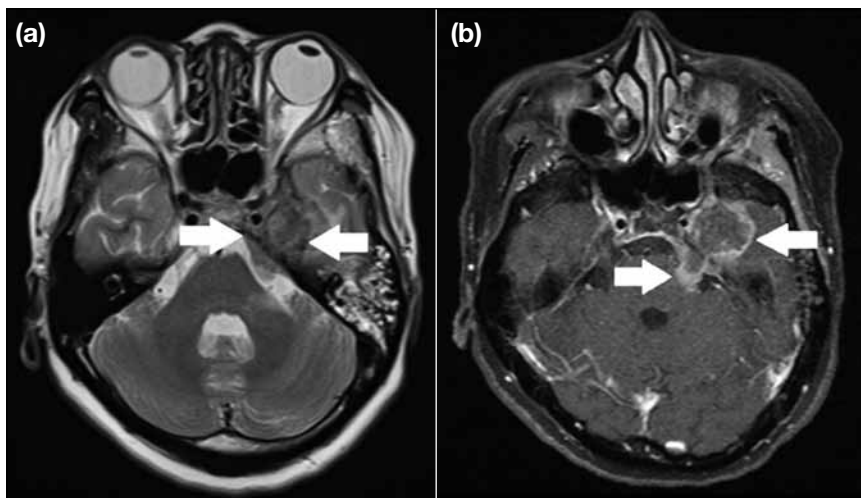


**Figure 2.** Neurolymphomatosis at trigeminal nerve. (a) Axial T2-weighted magnetic resonance image showing loss of normal cerebrospinal fluid signal at left Meckel's cave with nodular enlargement of the trigeminal nerve from the cisternal portion to the cavernous portion (white arrows). (b) Gadolinium-enhanced magnetic resonance image with fat suppression showing mild to moderate enhancement of the thickened left trigeminal nerve (white arrows). Findings are compatible with neurolymphomatosis, given the clinical context of disseminated diffuse large B-cell lymphoma. Subsequent follow-up magnetic resonance imaging shows interval improvement after chemotherapy (not shown).

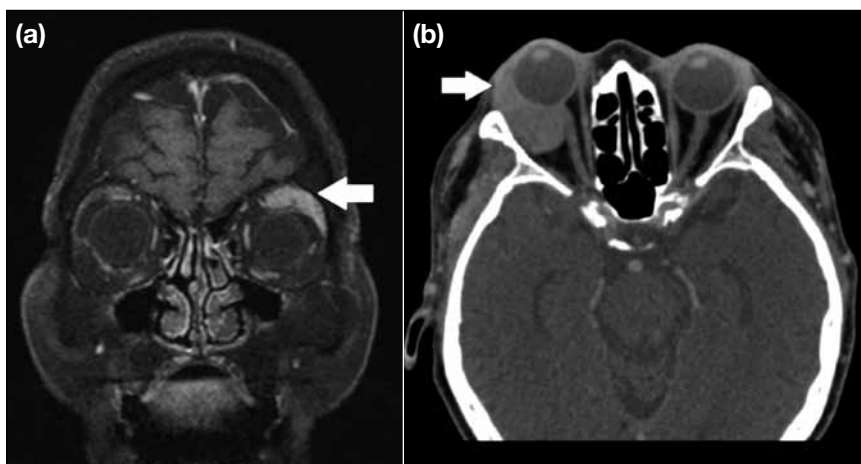


**Figure 3.** Primary orbital mucosa-associated lymphoid tissue lymphoma. (a) Coronal gadolinium-enhanced magnetic resonance image with fat suppression showing enlargement of left lacrimal gland. Subsequent incisional biopsy confirms mucosa-associated lymphoid tissue lymphoma. (b) A different patient with axial contrast-enhanced computed tomography of the orbit showing enlargement of the right lacrimal gland with mass effect causing proptosis. Computed tomography helps delineate the extent of retrobulbar involvement and shows intraconal extension abutting the optic nerve, alerting the ophthalmologist to be cautious when performing incisional biopsy. Pathology confirms mucosa-associated lymphoid tissue lymphoma.

is dichotomised into two distinct forms: diffuse and ill-defined versus smooth and circumscribed masses. Homogeneous enhancement of the mass is a characteristic feature of orbital lymphoma. Classically, these masses tend to demonstrate pliability and mould to normal orbital structures. Bone remodelling of the orbital walls as a result of this characteristic growth pattern is more common than osseous erosion.<sup>11</sup> Typical localisation of orbital lymphoma at the superolateral quadrant of the orbit may also aid in reaching a diagnosis (Figure 3).<sup>12</sup>

Cross-sectional imaging is helpful in delineating the exact extent of retrobulbar involvement, which is not readily assessed by clinical examination.

### **Salivary Glands**

Primary salivary gland lymphoma accounts for only 5% of extranodal non-Hodgkin lymphoma and 2% of salivary gland neoplasms.<sup>13</sup> The most common histological subtypes are mucosa-associated lymphoid tissue lymphoma, follicular B-cell lymphoma, and diffuse large B-cell lymphoma.<sup>13</sup> Salivary gland lymphoma can manifest as solitary or multiple lesions which sometimes demonstrate internal reticular pattern (Figure 4). Diffuse mixed solid-cystic appearance is commonly encountered in mucosa-associated lymphoid tissue lymphoma, whereas multiple solid masses are more common in other non-mucosa-associated lymphoid tissue lymphoma subtypes.<sup>13</sup> Distinction of lymphoma from other benign or malignant causes can be difficult as the imaging features are not pathognomonic for this condition. In cases of multiple masses, important differential diagnoses include inflammation, Sjögren syndrome, sarcoidosis, and metastases.<sup>14</sup>

## **MUSCULOSKELETAL SYSTEM**

### **Soft Tissue**

Cutaneous and subcutaneous soft tissue, as well as muscles, can be involved in lymphoma. Primary lymphoma of muscle is usually seen in adults aged >60 years and is predominantly B-cell-type lymphoma. The thigh, forearm, and back are the most commonly reported sites of occurrence.<sup>15</sup> Various radiological features are observed in skeletal muscle lymphoma, with muscle enlargement being common. Solitary or multiple focal muscle masses are frequently encountered, but this is relatively non-specific, because other differentials such as soft tissue sarcoma, metastasis, and haematoma can present similarly.<sup>16</sup> MRI is a valuable tool for assessment of this condition because it allows more detailed characterisation of soft

tissue signal abnormalities. In particular, long segmental signal abnormality or contrast enhancement along the direction of muscle fascicles has been suggested as a distinguishing feature of skeletal muscle lymphoma, and is rarely seen in other malignancies.<sup>15,17</sup> Apart from the more common diffuse contrast enhancement of the lymphomatous mass, predominantly peripheral thick band-like enhancement in the muscle and deep fascial enhancement can also be detected in skeletal muscle lymphoma, presumably the result of infiltrative multicompartamental involvement. This is in contrast to soft tissue sarcoma, which tends to be a compartmental condition.<sup>18</sup> However, this enhancement pattern can mimic necrotising fasciitis.<sup>17</sup> As such, caution in the imaging interpretation and correlation with the clinical picture is warranted. Spread along neurovascular bundle also suggests lymphoma rather than sarcoma, with the exception of epithelioid sarcoma which can demonstrate a similar pattern of spread.<sup>18</sup> Other associated features of skeletal muscle lymphoma include subcutaneous stranding, skin thickening, and intact traversing vessel; these are relatively typical for lymphoma as opposed to muscle sarcoma.

Imaging features of cutaneous and subcutaneous soft tissue lymphoma can be non-specific. They can demonstrate diffuse lymphomatous infiltration with skin thickening or focal mass in the soft tissue. Cross-sectional imaging can help detect any other body organ lymphomatous involvement.<sup>19,20</sup>

Diagnosis of soft tissue lymphoma can be hindered by a deceptive clinical presentation, because it can masquerade as an inflammatory condition such as cellulitis. In such circumstances, imaging plays an important role in the delineation of disease extent and in ruling out major complications of its mimics (eg, abscess formation in severe cellulitis). Thus, imaging helps direct clinicians to further investigation pathways, such as image-guided biopsy, to reach a definitive diagnosis (Figure 5).

### **Cranial Vault**

Primary cranial vault lymphoma is exceedingly rare. Common presenting symptoms are gradually enlarging scalp lump or headache from meningeal infiltration. Pericranium, meninges, and subcutaneous tissue of the scalp are involved in this condition. Radiologically, this is seen as a mass lesion centered at the cranial vault with intracranial and extracranial extension. Bone destruction is absent in most cases, because of the permeative growth of lymphoma, resulting in the appearance of a

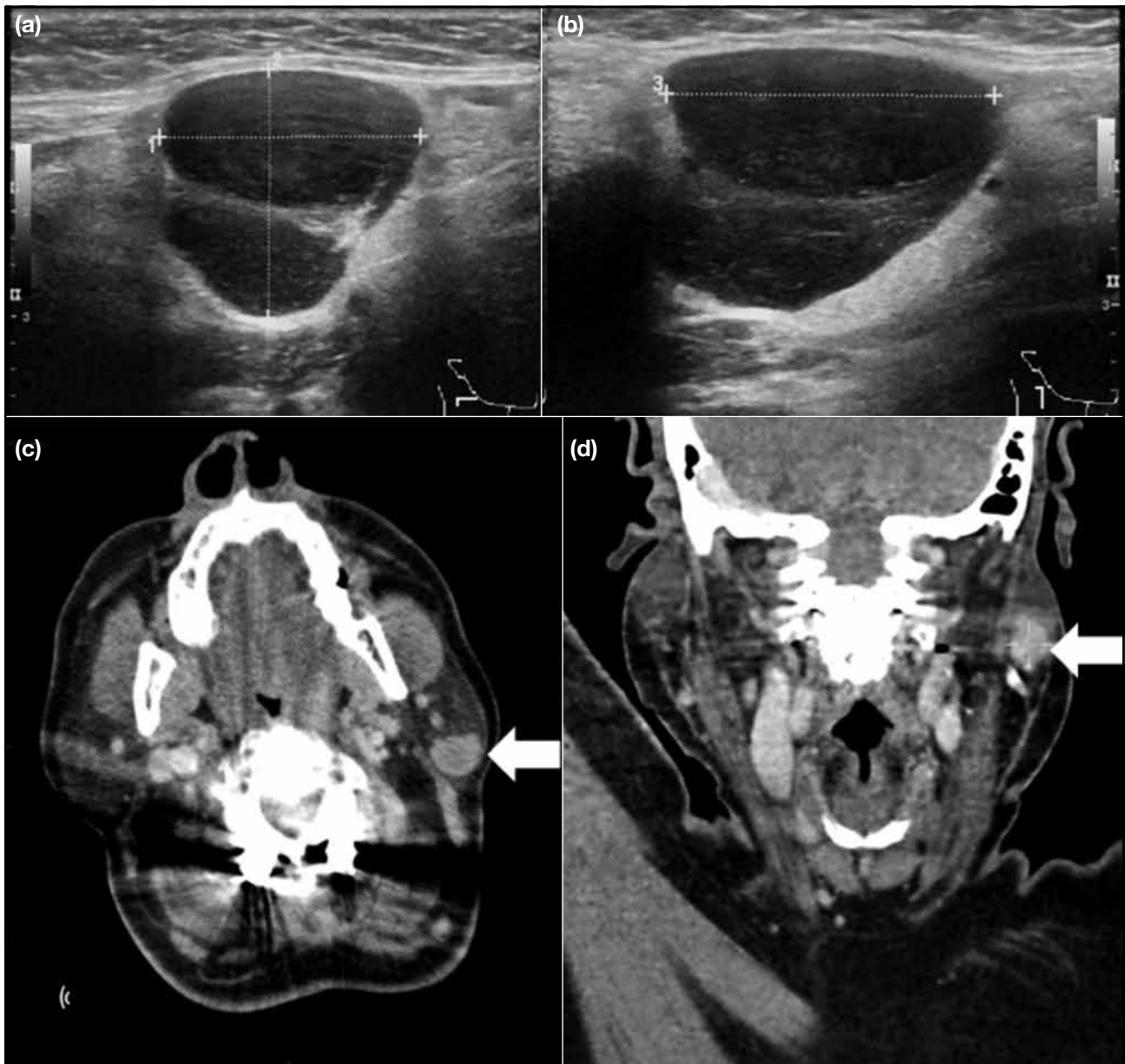


**Figure 4.** Primary salivary gland follicular lymphoma. (a) Transverse and (b) longitudinal greyscale ultrasonogram over the right submandibular gland shows a solitary intraglandular hypoechoic oval-shaped mass with internal reticular pattern. Appearance is suggestive of an abnormal lymph node with suspicion for lymphoma. Excisional biopsy confirms follicular lymphoma. Intraglandular lymph node involvement in lymphoma is considered as extranodal disease because this is not a defined nodal group. (c) Axial and (d) coronal contrast-enhanced computed tomography of neck in the same patient 1 year after the initial diagnosis showing a new solitary homogeneous mass (white arrows) in the left parotid gland. Subsequent biopsy of the lesion confirms recurrent follicular lymphoma.

large soft tissue mass with disproportionately little or absent aggressive bone changes (Figure 6).<sup>21</sup>

## THORAX Chest Wall

Primary chest wall lymphoma is rare; diffuse large B-cell lymphoma is the most common subtype of

the disease. Primary chest wall lymphoma can arise from the pleura and is thought to be associated with chronic pyothorax. Radiological features of primary chest wall lymphoma are non-specific, because a wide range of differentials exist for chest wall tumours, including other haematological malignancies such as myeloma. Primary chest wall lymphoma may show

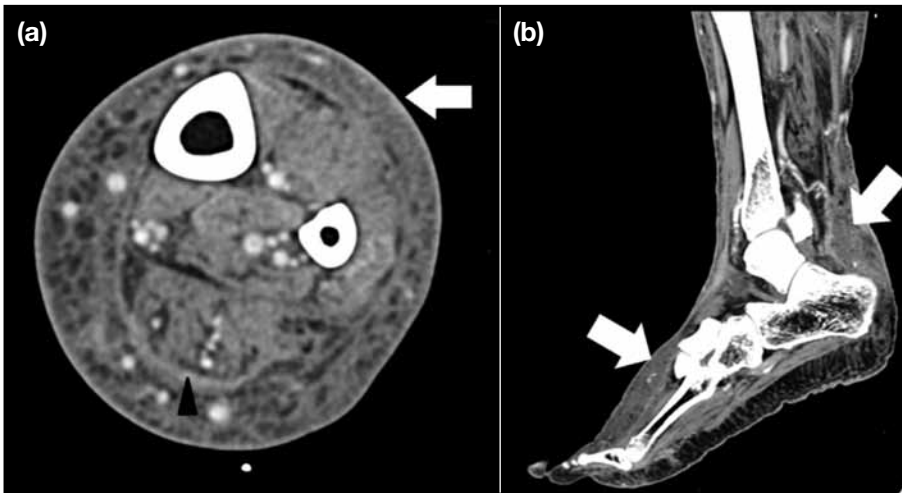


**Figure 5.** Primary musculoskeletal lymphoma. (a) Axial and (b) sagittal contrast-enhanced computed tomography of the left calf with clinically suspected severe cellulitis showing diffuse dermal thickening, prominent subcutaneous stranding (white arrow) and fascial thickening (black arrowhead). However, no sign of gangrene or abscess formation is detected on computed tomography. Subsequent incisional biopsy of the skin, fascia, and muscle shows highly aggressive extranodal nasal type natural killer / T-cell lymphoma.



**Figure 6.** Primary cranial vault lymphoma. (a) Frontal skull radiograph showing no focal skull vault destruction. (b) Coronal gadolinium-enhanced T1-weighted magnetic resonance image with fat suppression of the brain shows a large enhancing mass (white arrow) centring at left frontal bone with intracranial extra-axial component and extracranial subgaleal component while the intervening skull bone remains intact owing to permeative lymphomatous growth. (c) T2-weighted axial magnetic resonance image of the brain near vertex demonstrates T2 intermediate to low signal, suggesting highly cellular nature of lymphoma (white arrow). Biopsy of the mass confirms diffuse large B-cell lymphoma.

diffuse infiltration or have a multinodular appearance.<sup>22</sup> Pleural sandwich sign has been described as a helpful radiological feature of lymphomatous involvement in the pleura (Figure 7).<sup>23</sup>

### Breast

Primary breast lymphoma constitutes up to 0.7% of all breast malignancies; diffuse large B-cell lymphoma is the most common histological subtype.<sup>24</sup> It can present with single or multiple lesions. Common mammographic

findings in breast lymphoma are a non-calcified oval or round high-density mass with circumscribed or irregular margin (Figures 8a and 9a). It may also manifest as globally increased density in the affected breast. Sonographically, breast lymphoma can present with hypoechoic or mixed hyper- and hypo-echoic masses with vascularity and posterior enhancement, owing to its hypercellular nature (Figure 8b). Echogenic rim or onion peel-like rim may be seen, owing to surrounding lymphoedema (Figure 8c and 9b).<sup>24</sup>

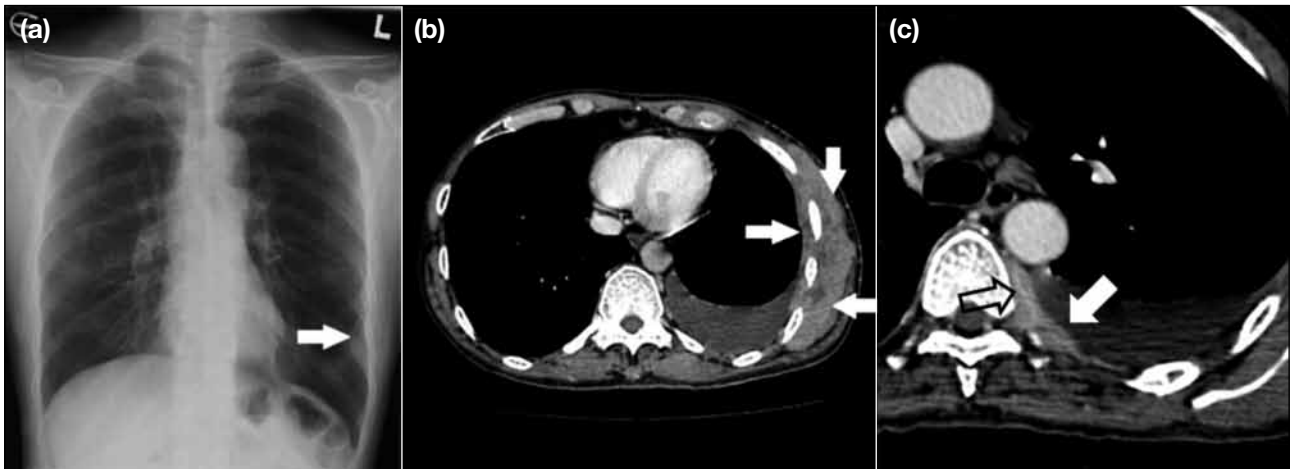


**Figure 7.** Primary chest wall lymphoma. (a) Chest radiograph shows a pleura-based mass at left lower lateral hemithorax (white arrow), taken several months before subsequent computed tomography (b and c). (b) Axial contrast-enhanced computed tomography thorax shows left pleural effusion and large left chest wall infiltrative mass (white arrows). (c) Another left pleural-based mass (white arrow) in a more superior section of the computed tomography shows an intercostal vessel (black empty arrow) traversing the lesion, giving the “pleural sandwich sign”. Biopsy of the mass shows diffuse large B-cell lymphoma.

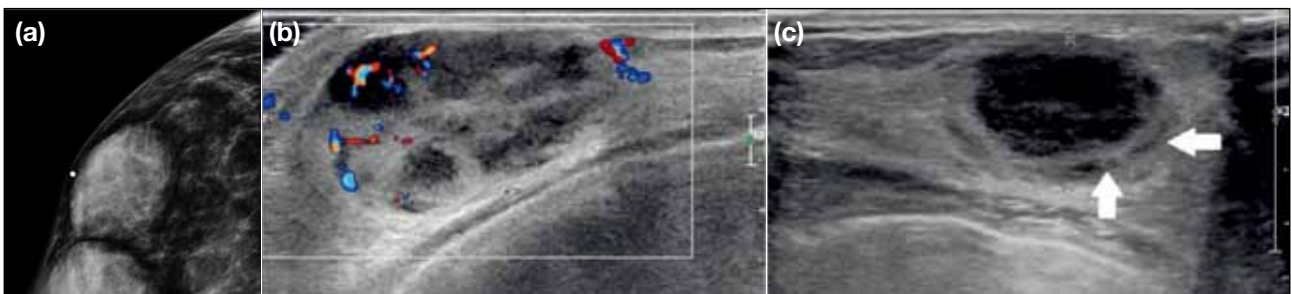


**Figure 8.** Breast lymphoma in a patient with disseminated recurrent lymphoma. (a) Right craniocaudal view mammogram showing multiple circumscribed masses in right breast with no calcification. (b) Doppler ultrasonogram of right breast mass showing mixed hyper- and hypo-echoic mass with intralesional vascularity. (c) Greyscale ultrasonogram showing hypoechoic mass with onion peel-like rim due to perifocal lymphoedema (white arrows). Posterior enhancement is evident, which is related to hypercellularity of the lesion.

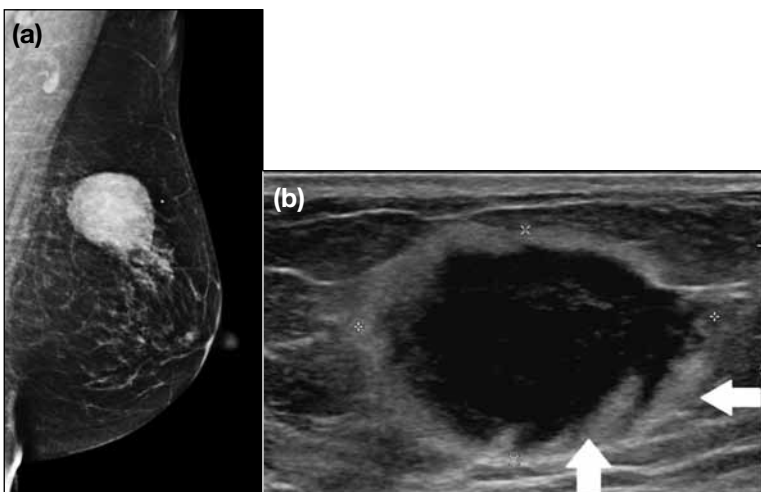


**Figure 9.** Primary breast lymphoma. (a) Left mediolateral oblique view mammogram showing single high-density left breast mass with partially obscured border. (b) Greyscale ultrasonogram showing echogenic rim of the lesion (white arrows) and posterior enhancement. Biopsy shows diffuse large B-cell lymphoma.

## ABDOMINAL Gastrointestinal Tract

Lymphoma in the gastrointestinal tract is quite common, accounting for 10% to 30% of all non-Hodgkin lymphoma. Gastrointestinal lymphoma is commonly mucosa-associated lymphoid tissue lymphoma. The stomach is the most common site of disease (Figure 10), followed by the small bowel

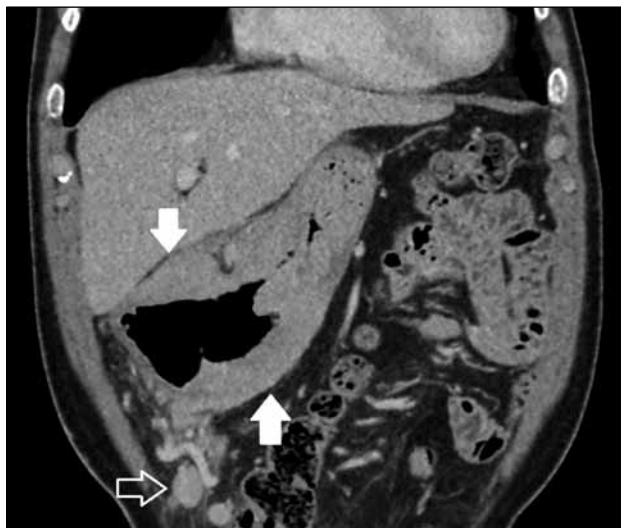


**Figure 10.** Primary gastric mucosa-associated lymphoid tissue lymphoma. Coronal contrast-enhanced computed tomography of the abdomen showing aneurysmal dilatation and circumferential wall thickening of the distal gastric body and antrum (white arrows) with enlarged perigastric lymph nodes (empty white arrow). Imaging features are typical of lymphoma.

(Figure 11), pharynx, large bowel (Figure 12), and oesophagus.<sup>25</sup> The common patterns of disease include circumferential wall thickening, aneurysmal dilatation of bowel loops and polypoid mass.<sup>25</sup> A key difference of gastrointestinal lymphoma, compared with the more common adenocarcinoma, is its non-obstructive nature. This difference is attributed to the lack of desmoplastic reaction and lymphomatous destruction of the myenteric plexus, which causes bowel dilatation instead of stricture. Compared with gastrointestinal tract adenocarcinoma, which is a mucosal disease process that can be more readily detectable at endoscopy, gastrointestinal tract lymphoma may be missed if the involvement is mainly submucosal or in a deep mucosal layer. Cross-sectional imaging therefore serves a superior role for mural and extraluminal evaluation in the detection of abnormal bowel wall feature and nodal mass, which may suggest lymphoma.<sup>26</sup>

## Liver and Spleen

Splenic involvement can be 20% to 40% of lymphoma, and hepatic involvement can be up to 15% of lymphoma.<sup>25</sup> Radiological patterns of lymphomatous involvement can be in the form of focal nodules or diffuse infiltration, and are non-specific (Figure 13). Focal nodules commonly appear well-defined and hypoechoic on sonography, and hypoenhancing relative to the rest of the normal parenchyma on contrast-enhanced CT. Solitary, multifocal, or even miliary nodules can be seen in hepatosplenic lymphomatous involvement.<sup>27,28</sup> In cases

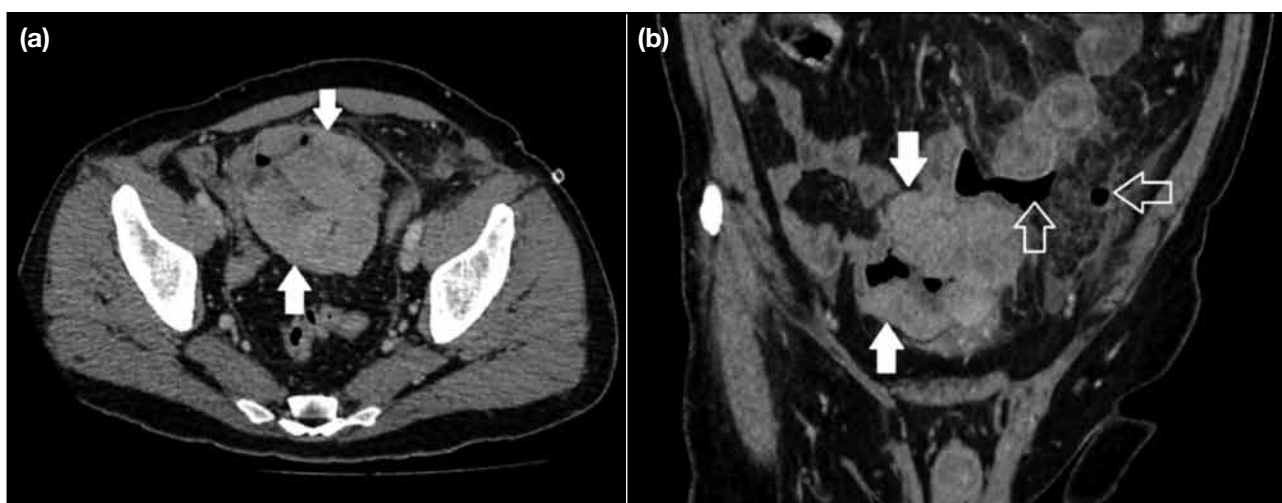


**Figure 11.** Primary small bowel lymphoma. (a) Axial contrast-enhanced computed tomography showing circumferential bowel wall thickening and aneurysmal dilatation of an ileal loop due to lymphomatous destruction of myenteric nerve plexus (white arrows). (b) Axial contrast-enhanced computed tomography showing similar findings (white arrows) as (a), with extraluminal gas (empty white arrows) suggesting perforation of the tumour.



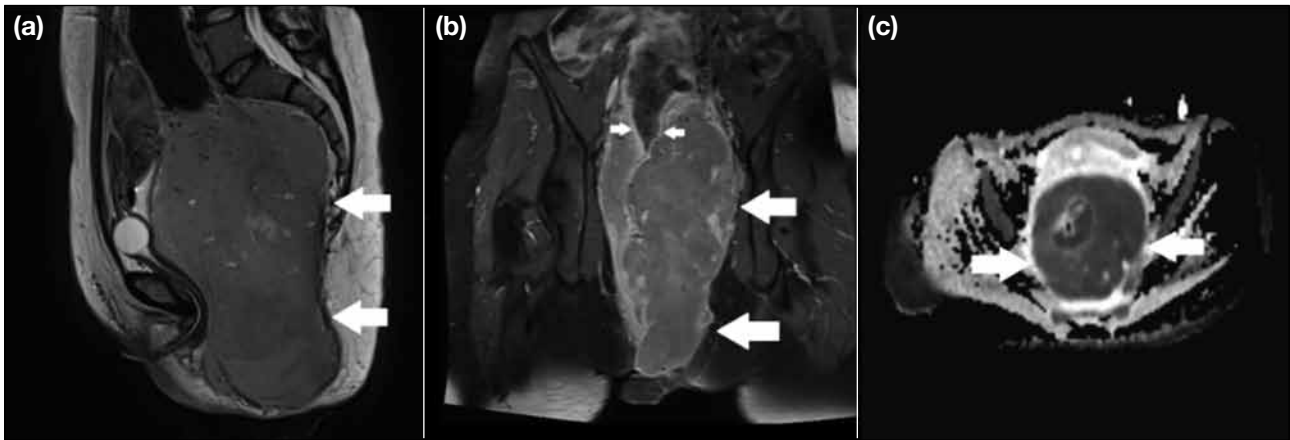


**Figure 12.** Primary rectal lymphoma. (a) Sagittal T2-weighted magnetic resonance image of the rectum showing a large T2 intermediate signal mass in the rectum (white arrows). (b) Oblique coronal gadolinium-enhanced T1-weighted magnetic resonance image with fat suppression showing relatively preserved mucosa (small white arrows) overlying the rectal mass (large white arrows) which is not typical of the more common adenocarcinoma of the rectum. (c) Axial apparent diffusion coefficient mapping of the rectum showing restricted diffusion of the tumour mass (white arrows). Biopsy confirms diffuse large B-cell lymphoma.



**Figure 13.** Hepatic lymphomatous involvement. Transverse greyscale ultrasonogram over the left lobe of the liver in a patient with disseminated high-grade diffuse large B-cell lymphoma. Disease involvement in the liver is evident by multifocal hypoechoic nodules. Imaging features are non-specific; clinical context and other investigations such as positron emission tomography-computed tomography would be necessary to confirm the diagnosis.



**Figure 14.** Renal lymphomatous involvement in a patient with disseminated lymphoma. Axial contrast-enhanced computed tomography showing focal left renal mass (white arrows) which is homogeneously hypoenhancing as compared with renal parenchyma, typical of hypovascular renal lymphoma. Subtle involvement is seen in the right kidney (empty white arrow).

of solitary hepatic lesion, the differentials of primary hepatic neoplasms (eg, hepatocellular carcinoma, intrahepatic cholangiocarcinoma, or focal nodular hyperplasia) and liver abscess should be considered.<sup>27</sup> Dedicated triphasic CT scan of the liver may help in differentiating other primary hepatic neoplasms from lymphoma by showing typical radiological features pertaining to the former entities. For differentiation from liver abscess, absence of perilesional oedema and

vascular thrombosis to suggest pylephlebitis, as well as presence of the “vessel penetration sign” with patent vessel traversing the lesion may suggest lymphoma.<sup>27</sup> In cases of multifocal lesions, important differential diagnoses are metastases and fungal abscesses.<sup>25</sup>

Periportal lymphomatous spread is a distinctive pattern of hepatic lymphomatous involvement, likely because the majority of lymphatic drainage of liver occurs via

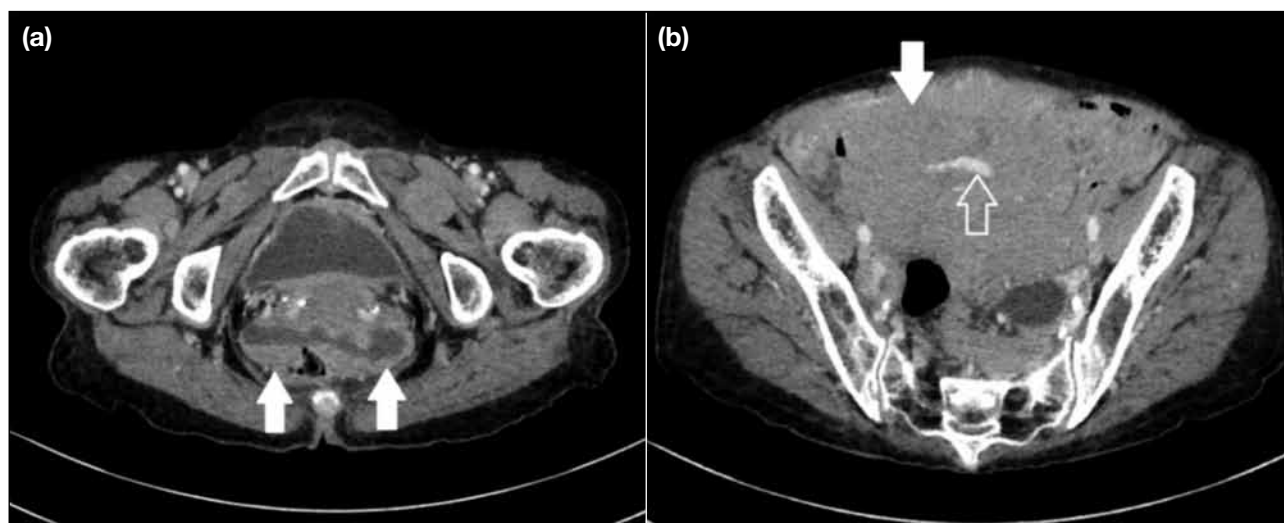


**Figure 15.** Peritoneal lymphomatosis. (a) Axial contrast-enhanced computed tomography showing peritoneal nodular thickening at rectovesical pouch (white arrows) and presence of ascites. (b) More superior section of the computed tomography showing large peritoneal mass (white arrow) with “sandwich sign” (empty white arrow) evidenced by the non-compressed traversing vessel within the mass.

the periportal lymphatic channels. Radiologically, periportal lymphomatous spread presents with periportal soft tissue cuffing or ill-defined masses.<sup>27</sup> Common differential considerations are periportal oedema (which can result from acute hepatitis, hepatic veno-occlusive disease, post-liver or bone marrow transplantation, fluid overload, congestive heart failure, and trauma), post-transplant lymphoproliferative disease (commonly after liver or pancreas transplantation), lymphadenopathy from other causes (eg, tuberculosis or viral hepatitis), or cholangiocarcinoma.<sup>29</sup>

### Kidney

Primary renal lymphoma is exceedingly rare. There are several common radiological patterns of renal lymphoma, including multiple roundish masses, contiguous spread from adjacent nodes, solitary mass, isolated perinephric mass and diffuse infiltration.<sup>25,30</sup> Renal lymphoma is typically hypovascular, which distinguishes it from the more common renal cell carcinoma (Figure 14). The lymphomatous masses in the kidneys are commonly homogeneous, iso- or hyper-dense to renal parenchyma in non-enhanced CT, and hypoenhancing in contrast-enhanced CT. The diffuse infiltrative pattern of renal lymphoma produces nephromegaly with preservation of overall reniform shape.<sup>30</sup>

### Peritoneum

Peritoneal lymphomatosis demonstrates peritoneal / omental masses and ascites (Figure 15). Important

imaging differentials include peritoneal carcinomatosis and tuberculous peritonitis. It is rarely encountered and may be seen in the setting of high-grade gastrointestinal non-Hodgkin lymphoma.<sup>25</sup>

### CONCLUSION

Various organs can be involved in lymphoma, but not all of them display diagnostic imaging features. Imaging plays an important role in documenting disease extent and in guiding biopsy for histological evaluation. Radiologists should recognise the multifaceted imaging spectrum of extranodal lymphoma, particularly the typical features of certain extranodal organ disease (eg, in the gastrointestinal tract, CNS, or kidneys) and consider lymphoma as differential in the appropriate context.

### REFERENCES

1. Leite NP, Kased N, Hanna RF, Brown MA, Pereira JM, Cunha R, et al. Cross-sectional imaging of extranodal involvement in abdominopelvic lymphoproliferative malignancies. *Radiographics*. 2007;27:1613-34. [Crossref](#)
2. Thomas AG, Vaidhyanath R, Kirke R, Rajesh A. Extranodal lymphoma from head to toe: part 1, the head and spine. *AJR Am J Roentgenol*. 2011;197:350-6. [Crossref](#)
3. Haldorsen IS, Espeland A, Larsson EM. Central nervous system lymphoma: characteristic findings on traditional and advanced imaging. *AJNR Am J Neuroradiol* 2011;32:984-92. [Crossref](#)
4. Haldorsen IS, Kråkenes J, Krossnes BK, Mella O, Espeland A. CT and MR imaging features of primary central nervous system lymphoma in Norway, 1989-2003. *AJNR Am J Neuroradiol*. 2009;30:744-51. [Crossref](#)
5. Smith AB, Smirniotopoulos JG, Rushing EJ. From the archives of the AFIP: central nervous system infections associated with

- human immunodeficiency virus infection: radiologic-pathologic correlation. *Radiographics*. 2008;28:2033-58. [Crossref](#)
6. Küker W, Nägele T, Korfel A, Heckl S, Thiel E, Bamberg M, et al. Primary central nervous system lymphomas (PCNSL): MRI features at presentation in 100 patients. *J Neurooncol*. 2005;72:169-77. [Crossref](#)
  7. Cho SK, Na DG, Ryoo JW, Roh HG, Moon CH, Byun HS, et al. Perfusion MR imaging: clinical utility for the differential diagnosis of various brain tumors. *Korean J Radiol*. 2002;3:171-9. [Crossref](#)
  8. Baehring JM, Batchelor TT. Diagnosis and management of neurolymphomatosis. *Cancer J*. 2012;18:463-8. [Crossref](#)
  9. Hughes RA, Britton T, Richards M. Effects of lymphoma on the peripheral nervous system. *J R Soc Med*. 1994;87:526-30.
  10. Amrami KK, Felmlee JP, Spinner RJ. MRI of peripheral nerves. *Neurosurg Clin N Am*. 2008;19:559-72,vi. [Crossref](#)
  11. Tailor TD, Gupta D, Dalley RW, Keene CD, Anzai Y. Orbital neoplasms in adults: clinical, radiologic, and pathologic review. *Radiographics*. 2013;33:1739-58. [Crossref](#)
  12. Priego G, Majos C, Climent F, Muntane A. Orbital lymphoma: imaging features and differential diagnosis. *Insights Imaging* 2012;3:337-44. [Crossref](#)
  13. Zhu L, Wang P, Yang J, Yu Q. Non-Hodgkin lymphoma involving the parotid gland: CT and MR imaging findings. *Dentomaxillofac Radiol*. 2013;42:20130046. [Crossref](#)
  14. Bialek EJ, Jakubowski W, Zajkowski P, Szopinski KT, Osmolski A. US of the major salivary glands: anatomy and spatial relationships, pathologic conditions, and pitfalls. *Radiographics*. 2006;26:745-63. [Crossref](#)
  15. Chun CW, Jee WH, Park HJ, Kim YJ, Park JM, Lee SH, et al. MRI features of skeletal muscle lymphoma. *AJR Am J Roentgenol*. 2010;195:1355-60. [Crossref](#)
  16. Hwang S. Imaging of lymphoma of the musculoskeletal system. *Radiol Clin North Am*. 2008;46:379-96. [Crossref](#)
  17. Lee VS, Martinez S, Coleman RE. Primary muscle lymphoma: clinical and imaging findings. *Radiology*. 1997;203:237-44. [Crossref](#)
  18. Suresh S, Saifuddin A, O'Donnell P. Lymphoma presenting as a musculoskeletal soft tissue mass: MRI findings in 24 cases. *Eur Radiol*. 2008;18:2628-34. [Crossref](#)
  19. Lim CY, Ong KO. Imaging of musculoskeletal lymphoma. *Cancer Imaging*. 2013;13:448-57. [Crossref](#)
  20. Lee HJ, Im JG, Goo JM, Kim KW, Choi BI, Chang KH, et al. Peripheral T-cell lymphoma: spectrum of imaging findings with clinical and pathologic features. *Radiographics*. 2003;23:7-26. [Crossref](#)
  21. Kantarci M, Erdem T, Alper F, Gundogdu C, Okur A, Aktas A. Imaging characteristics of diffuse primary cutaneous B-cell lymphoma of the cranial vault with orbital and brain invasion. *AJNR Am J Neuroradiol*. 2003;24:1324-6.
  22. Tateishi U, Gladish GW, Kusumoto M, Hasegawa T, Yokoyama R, Tsuchiya R, et al. Chest wall tumors: radiologic findings and pathologic correlation: part 2. Malignant tumors. *Radiographics*. 2003;23:1491-508. [Crossref](#)
  23. Kim Y, Lee M, Ryu Y, Cho MS. The pleural sandwich sign in two cases of primary pleural lymphoma. *Korean J Radiol*. 2015;16:213-6. [Crossref](#)
  24. Shim E, Song SE, Seo BK, Kim YS, Son GS. Lymphoma affecting the breast: a pictorial review of multimodal imaging findings. *J Breast Cancer*. 2013;16:254-65. [Crossref](#)
  25. Lee W, Lau E, Duddalwar VA, Stanley AJ, Ho YY. Abdominal manifestations of extranodal lymphoma: spectrum of imaging findings. *Am J Roentgenol*. 2008;191:198-206. [Crossref](#)
  26. Buy JN, Moss AA. Computed tomography of gastric lymphoma. *Am J Roentgenol*. 1982;138:859-65. [Crossref](#)
  27. Rajesh S, Bansal K, Sureka B, Patidar Y, Bihari C, Arora A. The imaging conundrum of hepatic lymphoma revisited. *Insights Imaging*. 2015;6:679-92. [Crossref](#)
  28. Saboo SS, Krajewski KM, O'Regan KN, et al. Spleen in haematological malignancies: spectrum of imaging findings. *Br J Radiol*. 2012;85:81-92. [Crossref](#)
  29. Tirumani SH, Shanbhogue AK, Vikram R, Prasad SR, Menias CO. Imaging of the porta hepatis: spectrum of disease. *RadioGraphics*. 2014;34:73-92. [Crossref](#)
  30. Urban BA, Fishman EK. Renal lymphoma: CT patterns with emphasis on helical CT. *RadioGraphics*. 2000;20:197-212. [Crossref](#)